

A quantum chemical mechanism for the water-initiated decomposition of silica

Janet E. Del Bene^{a,b,*}, Keith Runge^a, Rodney J. Bartlett^a

^a Quantum Theory Project, University of Florida, Gainesville, FL 32611, USA

^b Department of Chemistry, Youngstown State University, Youngstown, OH 44555, USA

Abstract

An ab initio quantum chemical investigation of the interaction of water with amorphous silica is carried out using model systems that contain the Si–O–Si bridging unit. Interaction of the silicon–oxygen bond with a water dimer is found to be most favorable, in contrast to the Michalske–Freiman model, which assumes that the interaction occurs with a single water molecule. Formation of a five-coordinated silicon atom is an essential intermediate in the bond fracture process, which involves proton transfer from the water dimer to the bridging oxygen, proton transfer within the water dimer, and the formation of a new Si–O bond. The activation barrier to rupture the Si–O bond in the Si–O–Si unit in the presence of water dimer is ~ 30 kcal/mol.

© 2002 Elsevier Science B.V. All rights reserved.

Keywords: Water; Silica; Water dimer; Hydrolytic weakening; Quantum mechanics; Ab initio quantum chemistry

1. Introduction

The fundamental event in the fracture of a covalently bonded material is the stress induced rupture of a chemical bond. In the case of amorphous silica, the crack tip velocity of a fracture is known to increase by orders of magnitude in the presence of water [1]. While the structure of amorphous silica is resilient to attack by water in an unstressed condition, stressing the solid leads to a weakening of the structure that is dependent on the concentration of water in the atmosphere. The

objective of this contribution is to use ab initio quantum chemistry to elucidate the mechanism by which water accomplishes this rupture.

The ability of quantum chemical calculations to describe the bond breaking process qualitatively, and quantitatively at sufficiently high levels of theory, is well established for small molecular systems [2]. However, ab initio quantum chemical calculations on large amorphous systems are not feasible. To develop a mechanistic understanding of the influence of chemical processes on bond rupture, it is appropriate to first study model systems to assess possible interactions. Others have explored the use of quantum chemical calculations on model systems to describe bond breaking in silica [3–7]. In this study, we have extended their investigations by employing more sophisticated models and improving the quantum mechanical

* Corresponding author. Address: Department of Chemistry, Youngstown State University, Youngstown, OH 44555, USA. Tel.: +1-330-742-3466; fax: +1-330-742-1579.

E-mail address: fr042008@ysub.yzu.edu (J.E. Del Bene).

treatment by including the effects of electron correlation and using larger and more flexible basis sets.

A number of theoretical approaches to the water–silica interaction have attempted to describe the nature of bond rupture based on insights gained from studies of the interaction of a single water molecule with the Si–O bond in a model compound [5–7]. The Michalske–Freiman model suggests an attack by a single water molecule at a crack tip. In this model, a lone pair of electrons on the water oxygen is oriented toward the silicon atom, and proton transfer occurs from water to the silica oxygen. This model has been computationally investigated on pyrosilicic acid ($\text{H}_6\text{Si}_2\text{O}_7$) by Lindsay et al. [7] using Hartree–Fock calculations on structures with constrained geometries. Although these calculations lend some support to the Michalske–Freiman model, the calculations themselves are limited by not including electron correlation effects, by the small basis sets used, and by the small number of restricted geometries that were sampled. In particular, the Si–O–Si arrangement was constrained to be linear, an arrangement that is rarely, if ever, found in the amorphous solid.

Bell and Dean [8] investigated the structure of amorphous silica using a random network of corner-sharing tetrahedra. Their analysis suggested that fourfold loops, which contain four silicon and four oxygen atoms, are required in order to reproduce the radial distribution functions available from experiment. West and Hench [6] reinvestigated the Michalske–Freiman model using three-, four- and fivefold silica rings as their model systems. A single water molecule was used to describe the interaction of water with the silica rings, employing the semi-empirical AM1 method for calculations on these relatively large systems. Such semi-empirical methods have known deficiencies: in particular, they tend to favor ring formation. The results of this study indicated that the interaction of a threefold ring with a single water molecule has the lowest activation barrier, and that straining the Si–O bond is essential to the fracture process. West and Hench also observed that a five-coordinate silicon is formed during the fracture process. However, the AM1 method that

they used for their study does not include d orbitals on silicon; hence the physics that underlie this five-coordinate silicon may not be properly described.

Gibbs [4] has described a set of early ab initio calculations on molecules used to model bonding in silicates. He suggested that changes in bond lengths and bond angles, charge densities, and force constants could be used as indicators of the suitability of a given system for modeling silica. In the present study we focus on bond length and angle variations as being key indicators of the fracture process. In particular, we examine the dependence of the fracture process on the nature of the interacting water species (monomer, dimer, trimer), the lengthening of an Si–O bond, and the bending of the Si–O–Si angle.

2. Methods

Full and constrained optimizations of selected model molecules and complexes were carried out at second-order perturbation theory [MBPT(2)] [9–12] with the 6–31 + G(d,p) basis set [13–16], a split-valence plus polarization basis augmented with diffuse functions on nonhydrogen atoms. This ab initio level of theory explicitly includes electron correlation effects at second-order, and has been shown to provide structures of hydrogen-bonded complexes in agreement with experimental data, as well as reasonable binding energies [17]. No basis set superposition error corrections have been made [18]. Optimized geometries were obtained for model molecules $\text{H}_3\text{Si-O-SiH}_3$, $\text{FH}_2\text{Si-O-SiFH}_2$, and $\text{F}_3\text{Si-O-SiF}_3$. These contain terminating groups with different electronegativities, thereby permitting an examination of the effect of these groups on the geometry of the bridging Si–O–Si linkage. Optimized geometries were also obtained for $\text{H}_3\text{Si-O-SiH}_3$ interacting with H_2O , $(\text{H}_2\text{O})_2$ and $(\text{H}_2\text{O})_3$ to explore the dependence of the water–silica interaction on the nature of the interacting water species. Since $\text{FH}_2\text{Si-O-SiFH}_2$ has an Si–O bond length which is closest to that observed in silica, and the SiFH_2 group should be fairly indicative of a terminating O in the extended silica system, we have selected this molecule as the model

for a detailed investigation of the water-initiated breakage of an Si–O bond. For this study, one Si–O bond ($\text{Si}_b\text{--O}$) in $\text{FH}_2\text{Si--O--SiFH}_2$ has been stretched and fixed during the subsequent optimization of the structure of a complex of this molecule and the water dimer. By systematically changing the value of the $\text{Si}_b\text{--O}$ distance, it has been possible to follow a reaction path for breakage of the Si–O bond. Since breakage of this bond leads to $\text{FH}_2\text{Si--OH}$ and $\text{FH}_2\text{Si--OH}$ hydrogen-bonded to H_2O , we have also optimized the structures of these moieties, requiring C_s symmetry in each, and the same conformation of the SiFH_2 groups that are found in the original complex. Systems that contain five-coordinated Si atoms, namely $\text{FH}_3\text{Si:OH}_2$ and $\text{F}_2\text{H}_2\text{Si:OH}_2$, have also been optimized. Calculations were carried out using Gaussian 98 [19] on the Cray SV1 computer at the Ohio Supercomputer Center.

3. Results and discussion

The optimized structures of $\text{H}_3\text{Si--O--SiH}_3$ with H_2O , $(\text{H}_2\text{O})_2$ and $(\text{H}_2\text{O})_3$ are shown in Figs. 1–3. Selected structural parameters are given in Table 1. In all of these complexes, the $\text{H}_3\text{Si--O--SiH}_3$ moiety has C_s symmetry, and the O and hydrogen-bonded H of each H_2O molecule have been con-

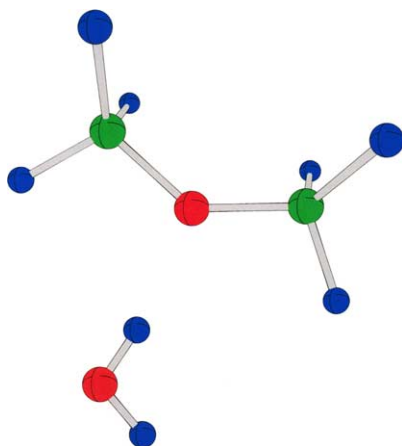


Fig. 1. Optimized structure of the complex of $\text{H}_3\text{Si--O--SiH}_3$ with one water molecule. Oxygens are shown in red, hydrogens in dark blue, and silicons in green.

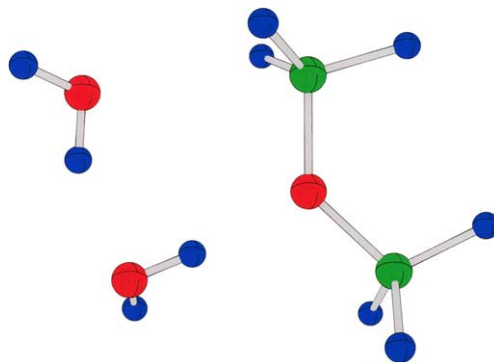


Fig. 2. Optimized structure of the complex of $\text{H}_3\text{Si--O--SiH}_3$ with the water dimer.

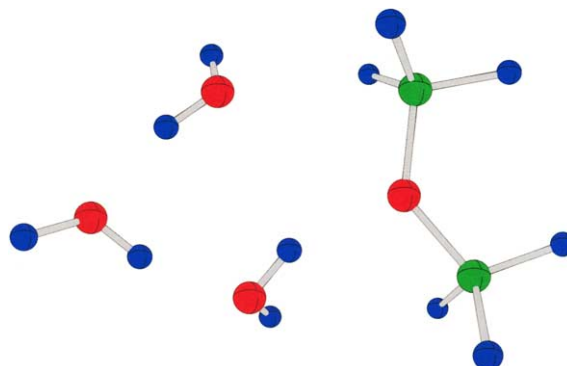


Fig. 3. Optimized structure of the complex of $\text{H}_3\text{Si--O--SiH}_3$ with the water trimer.

strained to lie in this plane. The other H atoms alternate above and below the plane. From Table 1, it can be seen that the $\text{Si}_a\text{--O}$ bond, which does not interact with water, appears to be insensitive to the presence of water. However, the $\text{Si}_b\text{--O}$ bond, which interacts with water, is longest when the interacting species is the water dimer. Moreover, contrary to the assumptions of Lindsay et al. [7], the introduction of any number of water molecules causes the Si–O–Si angle to bend toward a value closer to that found in amorphous silica. The binding energies of the complexes relative to the energies of the optimized water monomer, dimer, and trimer increase in the order monomer < trimer < dimer. Thus, these data suggest that, contrary to the Michalske–Freiman model, it is the

Table 1

Structures and binding energies of complexes of $\text{H}_3\text{Si-O-Si-H}_3$ with H_2O , $(\text{H}_2\text{O})_2$, and $(\text{H}_2\text{O})_3$ ^{a,b}

Complex	$\text{Si}_a\text{-O}$	$\text{Si}_b\text{-O}^c$	$\angle\text{Si}_a\text{-O-Si}_b$	ΔE^d
$\text{H}_3\text{Si-O-Si-H}_3:\text{OH}_2$	1.682	1.679	139.0	-4.4
$\text{H}_3\text{Si-O-Si-H}_3:(\text{H}_2\text{O})_2$	1.681	1.698	134.0	-6.4
$\text{H}_3\text{Si-O-Si-H}_3:(\text{H}_2\text{O})_3$	1.678	1.690	134.0	-3.7 ^e
	O-O^f	O-O^f	O-O^f	O-Si_b
$\text{H}_3\text{Si-O-Si-H}_3:\text{OH}_2$	2.926			3.705
$\text{H}_3\text{Si-O-Si-H}_3:(\text{H}_2\text{O})_2$	2.864	2.800		3.237
$\text{H}_3\text{Si-O-Si-H}_3:(\text{H}_2\text{O})_3$	2.890	2.766	2.804	3.062

^a Distances in Å; angles in degrees; binding energies in kcal/mol.^b The two rotamers of $\text{H}_3\text{Si-O-SiH}_3$ in which the SiH_3 groups may be staggered or eclipsed are essentially isoenergetic, differing by less than 0.1 kcal/mol. Both have a linear Si-O-Si arrangement, with Si-O bond lengths of 1.650 Å.^c The Si-O bond that interacts with water.^d The binding energies have been computed relative to $\text{H}_3\text{Si-O-Si-H}_3$ and the corresponding optimized water monomer, dimer, or trimer.^e The optimized water trimer is cyclic, with a binding energy of -18.6 kcal/mol. The trimer in the orientation found in the complex has a binding energy of -16.0 kcal/mol.^f The O-O and O-Si_b distances are listed in a clockwise manner in the hydrogen-bonding plane beginning with the O of $\text{H}_3\text{Si-O-SiH}_3$ and ending with the O-Si_b distance. (See Figs. 1–3.) The hydrogen-bonded O-H bonds are slightly elongated relative to H_2O , ranging from 0.969 to 0.978 Å. The O-H bond length in the monomer is 0.963 Å.

water dimer that is best suited to interact with an Si-O bond.

The optimized structures of the monomers $\text{H}_3\text{Si-O-SiH}_3$, $\text{FH}_2\text{Si-O-SiFH}_2$, and $\text{F}_3\text{Si-O-SiF}_3$ have linear Si-O-Si arrangements, with Si-O bond lengths of 1.650, 1.639, and 1.615 Å, respectively. Since the Si-O distance in $\text{FH}_2\text{Si-O-SiFH}_2$ is closest to that in amorphous silica, and since we have shown that it is the water dimer that is best suited to interact with an Si-O bond, we have employed $\text{FH}_2\text{Si-O-SiFH}_2:(\text{OH}_2)_2$ as the model to investigate the breaking of the $\text{Si}_b\text{-O}$ bond. Fig. 4

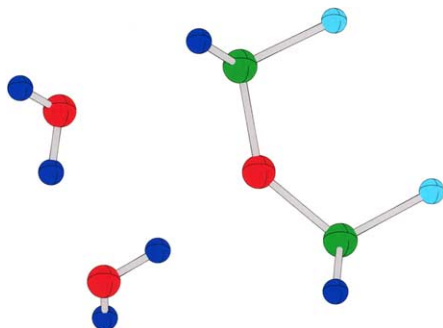


Fig. 4. Optimized structure of the complex of $\text{FH}_2\text{Si-O-SiH}_2\text{F}$ with the water dimer. Fluorine is shown in light blue.

presents the optimized structure of $\text{FH}_2\text{Si-O-SiFH}_2:(\text{H}_2\text{O})_2$. Selected structural parameters and binding energies for the optimized structures of $\text{FH}_2\text{Si-O-SiFH}_2$ and $\text{FH}_2\text{Si-O-SiFH}_2:(\text{H}_2\text{O})_2$ as a function of the length of the $\text{Si}_b\text{-O}$ bond are reported in Table 2, and illustrated graphically in Figs. 5–7. For these calculations, the fluorine atoms have been oriented trans to the approaching water dimer with respect to the Si-O bond.

Table 2

Structures of $\text{FH}_2\text{Si-O-SiFH}_2$ and structures and binding energies of complexes of $\text{FH}_2\text{Si-O-SiFH}_2$ with $(\text{H}_2\text{O})_2$ ^a

Complexes	$\text{Si}_a\text{-O}$	$\text{Si}_b\text{-O}$	$\angle\text{Si}_a\text{-O-Si}_b$	ΔE^b
Optimized	1.663	1.684	140.0	-11.9
<i>Optimized complexes with fixed $\text{Si}_b\text{-O}$</i>				
	1.662	1.75	137.0	-14.4
	1.660	1.85	134.0	-16.8
	1.658	1.95	132.0	-19.0
	1.656	2.05	130.0	-21.3
	1.653	2.15	129.0	-24.0
	1.677	2.50	139.0	-61.8
	1.668	2.70	138.0	-80.2

^a Distances in Å; angles in degrees.^b Binding energies in kcal/mol relative to the corresponding optimized $\text{FH}_2\text{Si-O-SiFH}_2$ monomer and two H_2O molecules.

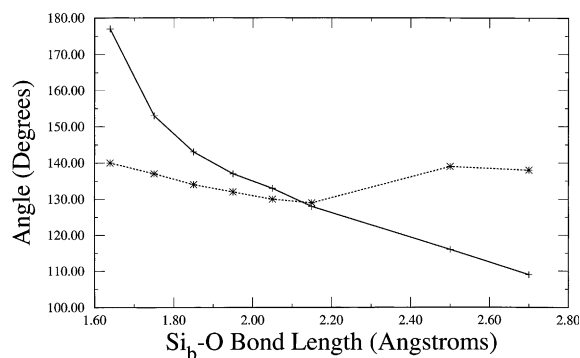


Fig. 5. Variation of the Si–O–Si angle with changes in the length of the Si_b–O bond, solid line: dry; dotted line: in the presence of the water dimer.

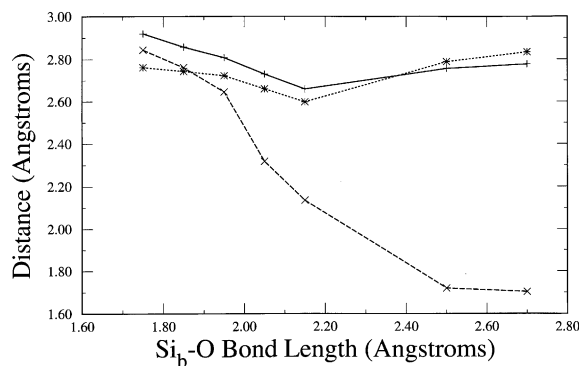


Fig. 6. Dependence of selected oxygen–oxygen and silicon–oxygen distances on the Si_b–O distance. O_b is the oxygen of the Si–O–Si bridge; O_{wb} is the oxygen of the water dimer proton-acceptor molecule that approaches the bridging oxygen at equilibrium; O_{ws} is the water oxygen of the proton-donor water molecule in the dimer that is closer to Si_b at equilibrium. Solid line: O_b–O_{wb}, dotted line: O_b–O_{ws}, dashed line: Si_b–O_{ws}.

It is apparent from Fig. 5 that even in the absence of the water dimer, as the Si_b–O bond length increases the Si–O–Si bending angle decreases, eventually reaching the tetrahedral value. In the presence of the water dimer, the bending angle again decreases, but only to 130°. As the Si_b–O bond length increases the ring defined by the hydrogen-bonded O and H atoms of the water dimer, the Si_b atom, and the oxygen of the Si–O–Si bridge, contracts. Thus, for the Si–O bond to rupture requires that the lengthening of the Si–O bond be accompanied by a sufficiently close approach of the water dimer to facilitate a double

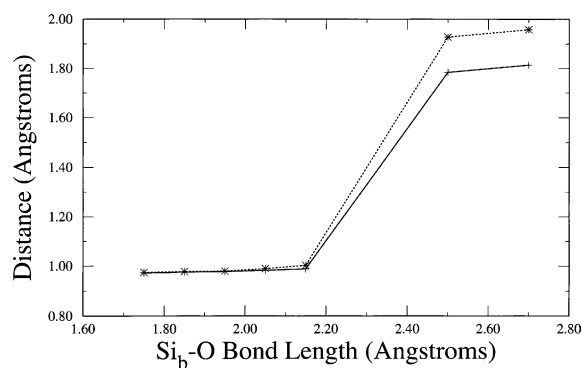


Fig. 7. Dependence of selected hydrogen-bonded O–H distances in the original water dimer on the length of the Si_b–O bond. Solid line: O_{wb}–H, dotted line: O_{ws}–H.

proton transfer. At an Si_b–O distance of 2.50 Å, proton transfer occurs from the O–H of the proton-acceptor water molecule in the original water dimer to the O of Si–O–Si. At the same time, the hydrogen-bonded proton in the original proton-donor molecule of the water dimer is transferred to the original proton acceptor oxygen. The remaining O–H group from the original proton-donor water molecule in the water dimer is now bonded to Si_b.

It is the water dimer that is ideally suited to effectively bridge the Si_b–O bond, and interact with it. Fig. 6 shows the changes in the distance between the bridging oxygen and the oxygen (O_{wb}) of the proton-acceptor water molecule in the water dimer, the distance between the Si_b atom and the oxygen (O_{ws}) of the proton-donor water molecule in the water dimer, and the O_{wb}–O_{ws} distance as a function of the Si_b–O distance. The O–O distances initially decrease and then increase slightly as the Si_b–O bond increases, and subsequently ruptures. In this process, the oxygen of the proton-donor water donates a pair of electrons to Si_b to form a new Si_b–OH bond, a proton is transferred to the oxygen of the Si–O–Si bridge, and a second proton is transferred within the water dimer. Fig. 7 illustrates graphically the changes in O–H distances during this process. As is evident from this figure, two hydrogen atoms that were bonded to oxygens in the original water dimer are no longer bound to these same oxygens after rupture of the Si_b–O bond.

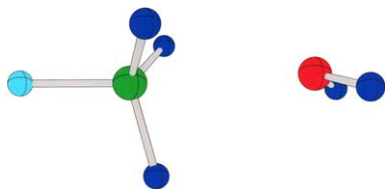


Fig. 8. The five-coordinated silicon complex $\text{FSiH}_3\text{:OH}_2$. Colors are defined in Figs. 1 and 4.

At an $\text{Si}_b\text{--O}$ distance of 2.70 Å, the products of bond breakage are evident. These are FH_2SiOH and FH_2SiOH hydrogen-bonded to one water molecule [$\text{FH}_2\text{SiOH}\text{:OH}_2$]. The activation barrier for bond breaking in the presence of water dimer is about 30 kcal/mol, significantly less than the barrier for the dry fracture of the same bond, which is more than 100 kcal/mol. Since one O–H of this water molecule had been constrained to lie in the Si–O–Si plane, the structure of the resulting hydrogen-bonded complex is not an optimized structure. Nevertheless, the energy of the $\text{FH}_2\text{SiOH}\text{:}(\text{OH}_2)_2$ system at an $\text{Si}_b\text{--O}$ distance of 2.70 Å is only 6.3 kcal/mol greater than the sum of the energies of the corresponding optimized $\text{FH}_2\text{SiOH}\text{:OH}_2$ and FH_2SiOH_2 . Thus, it is the insertion of water dimer, rather than a single water molecule, that appears to be essential for describing the breaking of an Si–O bond.

Fig. 8 shows one of the two five-coordinate silicon species, $\text{FH}_3\text{Si}\text{:OH}_2$ and, $\text{F}_2\text{H}_2\text{Si}\text{:OH}_2$, that have also been investigated in this study. The basis

Table 3
Selected distances (Å) and binding energies (kcal/mol) of five-coordinated Si species $\text{FH}_3\text{Si}\text{:OH}_2$ and $\text{F}_2\text{H}_2\text{Si}\text{:OH}_2^a$

	Si–F ^b	Si–X ^c	Si–O	ΔE
$\text{FH}_3\text{Si}\text{:OH}_2$	1.648	1.467	2.788	–4.9 ^d
$\text{F}_2\text{H}_2\text{Si}\text{:OH}_2$	1.629	1.628	2.796	–5.8 ^e

^a These molecules have slightly distorted trigonal bipyramidal structures (see Fig. 5). They are equilibrium structures (no imaginary frequencies) on their potential surfaces.

^b The axial Si–F bond.

^c The equatorial in-plane Si–H bond in $\text{FH}_3\text{Si}\text{:OH}_2$ and the equatorial Si–F bond in $\text{F}_2\text{H}_2\text{Si}\text{:OH}_2$.

^d The binding energy computed relative to SiFH_3 and H_2O .

^e The binding energy computed relative to SiF_2H_2 and H_2O .

set that has been used includes d orbitals, which are necessary for a physically meaningful description of silicon hypervalency. Table 3 shows selected geometric parameters and binding energies for these two five-coordinate silicon moieties, both of which are equilibrium structures on their potential surfaces. The formation of such structures appears to be a vital intermediate step in the breaking of the Si–O bond, as evident from the structures of the complexes reported above.

4. Conclusions

In this study we have investigated the structures and energies of complexes in which an Si–O bond interacts with water in order to elucidate the mechanism of the water-induced rupture of this bond in silica. The introduction of strain in the Si–O bond leads to a bending of the Si–O–Si angle toward a value consistent with that found in the amorphous solid. This bending is also induced by the presence of one, two or three water molecules.

Complexes in which water monomer, dimer, and trimer are bound to molecules with an Si–O–Si bridge are bound relative to the isolated species. However, the binding energy for the dimer is largest. The approach of the water dimer to an Si–O bond in an Si–O–Si bridge leads to breakage of one Si–O bond, the formation of a new Si–O bond, and the transfer of two protons. The activation barrier to this process is approximately 30 kcal/mol, significantly lower than the barrier in the absence of water. This result challenges the conventionally accepted model of Mechalske and Freiman, which postulates that Si–O bond rupture occurs through the interaction of an Si–O bond with a single water molecule. A substantial atomic rearrangement accompanies the rupture of the Si–O bond, and this rearrangement appears to be concerted.

A five-coordinated silicon atom is formed during the process of stress-initiated fracture of silica. The incorporation of the water dimer, a five-coordinate silicon, and appropriate atomic rearrangements which are part of the bond breaking process poses a challenging task for a physically realistic molecular dynamics simulation of the

fracture of silica in the presence, or absence, of water.

Acknowledgements

This work is supported by NSF Grant no. DMR 9980015.

References

- [1] S.M. Wiederhorn, *J. Am. Ceram. Soc.* 50 (1967) 407.
- [2] R.J. Bartlett, in: D.R. Yarkony (Ed.), *Modern Electronic Structure Theory*, World Scientific Publishing Co. Ltd., Singapore, 1995.
- [3] T.A. Michalske, S.W. Freiman, *J. Am. Ceram. Soc.* 66 (1983) 284.
- [4] G.V. Gibbs, *Am. Mineral.* 67 (1982) 421;
A.C. Lasaga, G.V. Gibbs, *Phys. Chem. Miner.* 14 (1987) 107;
A.C. Lasaga, G.V. Gibbs, *Phys. Chem. Miner.* 16 (1988) 29.
- [5] N.L. Ross, E.P. Meagher, *Am. Mineral.* 69 (1984) 1145.
- [6] J.K. West, L.L. Hench, *J. Mater. Sci.* 29 (1994) 5808.
- [7] C.G. Lindsay, G.S. White, S.W. Freiman, W. Wong-Ng, *J. Am. Ceram. Soc.* 77 (1994) 2179.
- [8] R.J. Bell, P. Dean, *Philos. Mag.* 25 (1972) 1381.
- [9] R.J. Bartlett, D.M. Silver, *J. Chem. Phys.* 62 (1975) 3258.
- [10] J.A. Pople, J.S. Binkley, R. Seeger, *Int. J. Quantum Chem. Quantum Chem. Symp.* 10 (1976) 1.
- [11] R. Krishnan, J.A. Pople, *Int. J. Quantum Chem.* 14 (1978) 91.
- [12] R.J. Bartlett, G.D. Purvis, *Int. J. Quantum Chem.* 14 (1978) 561.
- [13] W.J. Hehre, R. Ditchfield, J.A. Pople, *J. Chem. Phys.* 56 (1972) 2257.
- [14] P.C. Hariharan, J.A. Pople, *Theor. Chim. Acta* 28 (1973) 213.
- [15] G.W. Spitznagel, T. Clark, J. Chandrasekhar, P.v.R. Schleyer, *J. Comput. Chem.* 3 (1983) 3633.
- [16] T. Clark, J. Chandrasekhar, G.W. Spitznagel, P.v.R. Schleyer, *J. Comput. Chem.* 4 (1983) 294.
- [17] J.E. Del Bene, Hydrogen bonding 1, in: P.v.R. Schleyer, N.L. Allinger, T. Clark, J. Gasteiger, P.A. Kollman, H.F. Schaefer III, P.R. Schreiner (Eds.), *Encyclopedia of Computational Quantum Chemistry*, vol. 2, Wiley, Chichester, UK, 1998.
- [18] T.H. Dunning Jr., *J. Phys. Chem. A* 104 (2000) 9062.
- [19] M.J. Frisch, G.W. Trucks, H.B. Schlegel, G.E. Scuseria, M.A. Robb, J.R. Cheeseman, V.G. Zakrzewski, J.A. Montgomery Jr., R.E. Stratmann, J.C. Burant, S. Dapprich, J.M. Millam, A.D. Daniels, K.N. Kudin, M.C. Strain, O. Farkas, J. Tomasi, V. Barone, M. Cossi, R. Cammi, B. Mennucci, C. Pomelli, C. Adamo, S. Clifford, J. Ochterski, G.A. Petersson, P.Y. Ayala, J. Cui, K. Morokuma, D.K. Malick, A.D. Rabuck, K. Raghavachari, J.B. Foresman, J. Cioslowski, J.V. Ortiz, A.G. Baboul, B.B. Stefanov, G. Liu, A. Liashenko, P. Piskorz, I. Komaromi, R. Gomperts, R.L. Martin, D.J. Fox, T. Keith, M.A. Al-Laham, C.Y. Peng, A. Nanayakkara, C. Gonzalez, M. Challacombe, P.M.W. Gill, B. Johnson, W. Chen, M.W. Wong, J.L. Andres, C. Gonzalez, M. Head-Gordon, E.S. Replogle, J.A. Pople, *Gaussian 98*, Gaussian, Inc., Pittsburgh, PA 1998.